Renal Ultrafiltration Changes Induced by Focused US[1]

Krisztina Fischer, MD
Nathan J. McDannold, PhD
Yongzhi Zhang, MD
Magdolna Kardos, MD
Andras Szabo, MD
Antal Szabo, DSc
Gyorgy S. Reusz, MD
Ferenc A. Jolesz, MD

Purpose: To determine if focused ultrasonography (US) combined with a diagnostic microbubble-based US contrast agent can be used to modulate glomerular ultrafiltration and size selectivity.

Materials and Methods: The experiments were approved by the animal care committee. The left kidney of 17 healthy rabbits was sonicated by using a 260-kHz focused US transducer in the presence of a microbubble-based US contrast agent. The right kidney served as the control. Three acoustic power levels were applied: 0.4 W (six rabbits), 0.9 W (six rabbits), and 1.7 W (five rabbits). Three rabbits were not treated with focused US and served as control animals. The authors evaluated changes in glomerular size selectivity by measuring the clearance rates of 3000- and 70 000-Da fluorescence-neutral dextrans. The creatinine clearance was calculated for estimation of the glomerular filtration rate. The urinary protein-creatinine ratio was monitored during the experiments. The authors assessed tubular function by evaluating the fractional sodium excretion, tubular reabsorption of phosphate, and γ-glutamyltransferase–creatinine ratio. Whole-kidney histologic analysis was performed. For each measurement, the values obtained before and after sonication were compared by using the paired *t* test.

Results: Significant ($P < .05$) increases in the relative (ratio of treated kidney value/nontreated kidney value) clearance of small- and large-molecule agents and the urine flow rates that resulted from the focused US treatments were observed. Overall, 1.23-, 1.23-, 1.61-, and 1.47-fold enhancement of creatinine clearance, 3000-Da dextran clearance, 70 000-Da dextran clearance, and urine flow rate, respectively, were observed. Focal tubular hemorrhage and transient functional tubular alterations were observed at only the highest (1.7-W) acoustic power level tested.

Conclusion: Glomerular ultrafiltration and size selectivity can be temporarily modified with simultaneous application of US and microbubbles. This method could offer new opportunities for treatment of renal disease.

Supplemental material: *http://radiology.rsna.org/lookup/suppl/doi:10.1148/radiol.2532082100/-/DC1*

[1] From the Department of Radiology, Brigham and Women's Hospital, Harvard Medical School, Focused Ultrasound Laboratory, 221 Longwood Ave, Room 515, Boston, MA 02215 (K.F., N.J.M., Y.Z., F.A.J.); and 2nd Department of Pathology (M.K.) and 1st Department of Pediatrics (K.F., Andras Szabo, Antal Szabo, G.S.R.), Semmelweis University, Budapest, Hungary. Received November 26, 2008; revision requested January 9, 2009; revision received March 26; accepted April 29; final version accepted May 19. Supported in part by CIMIT New Concept Award. **Address correspondence to** K.F. (e-mail: *kfischer@bwh.harvard.edu*).

Various ultrasonographically (US) generated acoustic mechanical effects can induce transient changes in cell permeability and function (1–3). These effects, often termed *sonoporations,* can be enhanced with a microbubble-based US contrast agent (4) and have been tested as possible methods of enhancing the delivery of drugs and genes.

US combined with microbubbles can also be used to enhance vascular permeability. Low-intensity focused US (hereafter, focused US) exposures (ie, sonications) combined with the administration of gas microbubble–based diagnostic US contrast agents have been shown to temporarily disrupt the blood-brain barrier (5–11). Although the exact mechanism underlying this disruption is unknown, it appears that the sonications increase both passive and active transport mechanisms (7,12) and induce physiologic changes—namely, temporary vasospasms (13).

The glomerulus is another vascular structure that acts as a barrier between the blood and the formative urine. Glomerular ultrafiltration is a hemodynamically regulated event that is modulated through the glomerular barrier (14). This barrier has physical properties that can be dynamically changed. These properties include the thickness and charge of the glomerular basement membrane and the spread of the epithelial layer of the slit diaphragm to increase or decrease the glomerular ultrafiltration coefficient, as needed, to reach filtration pressure equilibrium (15–18). Our purpose in this study was to determine if focused US combined with a diagnostic microbubble-based US contrast agent can be used to modulate glomerular ultrafiltration and size selectivity.

Advances in Knowledge

- Focused US with simultaneous administration of a US microbubble-based contrast agent can noninvasively induce temporary glomerular filtration rate enhancement in healthy rabbits and thus is potentially applicable to injured kidney function.
- Focused US treatment in the presence of microbubbles enhances the clearance of large-molecule agents—herein 70 000-Da dextran—that normally are not cleared from the kidney.

Materials and Methods

All procedures performed in the animal experiments were approved by the institutional animal care committee of Harvard Medical Area. We treated the exposed left kidney of 17 healthy rabbits with focused US and a microbubble-based US contrast agent (10 μL/kg perflutren lipid microspheres, Definity; Bristol-Myers Squibb Medical Imaging, North Billerica, Mass). The right kidney served as the control. Three acoustic power levels were applied: 0.4 W (six rabbits), 0.9 W (six rabbits), and 1.7 W (five rabbits). Three rabbits were not treated with focused US and served as control animals, and one of these rabbits was injected with the US contrast agent. Figures 1 and 2 show the experimental setup and the experimental timeline, respectively.

Animal Preparation

Twenty male New Zealand white rabbits weighing 3000–3500 g were anesthetized with a mixture of xylazine (12 mg/kg/hr) and ketamine (48 mg/kg/hr). Saline solution infusion (1 mL/min) was started after anesthesia was induced. The left kidney was surgically exposed for easy targeting by the acoustic beam. Left-kidney urine was collected from the bladder with use of a Foley catheter placed in the urethra. The ureter of the right kidney was cut, and a ureter catheter (Kendall Tyco Healthcare; Mansfield, Mass) was inserted for collection of right-kidney urine. Blood pressure was continuously monitored during the procedure by using a polygraph (model 7D; Grass Instruments, Quincy, Mass) via a cannula placed in the carotid artery. A catheter for intravenous injection was placed in the left ear vein.

Experimental Setup

The focused US transducer was housed in a manually operated mechanical positioning system and submerged in a tank of degassed deionized water (Fig 1). The animal lay on its side on a plastic tray that had a 3 × 5-cm rectangular hole cut in it and was mounted on the top of the tank. A thin plastic sheet was loosely attached to the top of the tray and pushed through the rectangular hole to form a bag that was filled with degassed water, the temperature of which was monitored and maintained at about 37°C with use of a heating coil. The exposed left kidney hung in the water bag. The bottom of the water bag rested on a taut, acoustically transparent plastic membrane that was mounted below it.

US Procedure

The acoustic fields were generated with an air-backed, spherically curved transducer (frequency, 260 kHz; curvature diameter, 10 cm; curvature radius, 8 cm) that was manufactured in-house. The transducer was powered by a function generator (model 276; Fluke, Everett, Wash) and a radiofrequency amplifier (model 240L; E & I, Rochester, NY). Electrical power was measured with a power meter (model E419B; Agilent, Santa Clara, Calif) and a dual directional coupler (model C5948-10; Werlatone, Brewster, NY). Methods used to characterize the transducer are described elsewhere (19). The half-intensity beam diameter and the length of the focal spot were 8 and 40 mm, respectively, as mea-

Published online before print
10.1148/radiol.2532082100

Radiology 2009; 253:697–705

Abbreviation:
GFR = glomerular filtration rate

Author contributions:
Guarantors of integrity of entire study, K.F., N.J.M., Antal Szabo; study concepts/study design or data acquisition or data analysis/interpretation, all authors; manuscript drafting or manuscript revision for important intellectual content, all authors; manuscript final version approval, all authors; literature research, K.F., Y.Z., Andras Szabo, F.A.J.; experimental studies, K.F., N.J.M., Y.Z., M.K., Antal Szabo, F.A.J.; statistical analysis, K.F., G.S.R., F.A.J.; and manuscript editing, K.F., N.J.M., Y.Z., M.K., Andras Szabo, G.S.R., F.A.J.

Funding:
This research was supported by National Institutes of Health (grants U41 RR019703 and P01CA067165).

Authors stated no financial relationship to disclose.

sured in beam plots of the pressure amplitude squared. With such a long focal length, it was assumed that any US effects would occur through the entire thickness of the kidney within the focal spot. The frequency was selected on the basis of previous research of US-induced blood-brain barrier disruption, which revealed that lower frequencies result in less hemorrhage (20). The large size of the focal spot at this frequency also enabled us to target a fairly large portion of the kidney within a reasonable amount of time with use of our manual positioning system.

Each sonication consisted of 30 10-msec pulses at a repetition frequency of 1 Hz. The targets were located approximately 1 cm deep into the kidney in a single plane. Fifteen targets were sonicated at 1-cm intervals to encompass the extent of the 3 × 5-cm rectangular hole through which the kidney was hanging (Fig 1). As can be seen in the inset in Figure 1, some of the sonications were not in the kidney and were in the water only. We estimate that we targeted approximately 50% of the kidney volume. This approximation was based on measurements made on magnetic resonance images of a rabbit kidney in an unrelated (nonpublished) study and assumptions that the diameter of the affected area at each sonication was equal to the half-intensity beam diameter (8 mm) and the entire thickness of the kidney was affected along the direction of the focused ultrasound beam. Three acoustic power levels were tested: 0.4, 0.9, and 1.7 W. These exposure levels corresponded to negative pressure amplitudes (spatial peak, temporal peak estimates) of 0.30, 0.41, and 0.58 MPa in the focal plane, respectively, with the assumption of an acoustic attenuation of 6.5 Nepers/m/MHz (with use of average of values in a previous study [21]).

A bolus of US contrast agent (perflutren lipid microspheres) was injected intravenously at a dose of 10 μL/kg at the start of each of the 15 sonications and was followed by a 2-mL saline solution injection to flush the agent from the catheter. A delay between sonications of approximately 2 minutes allowed most of the bubbles to clear from the circulation. A hydrophone was used to monitor acoustic emission during sonication (Appendix E1, *http://radiology.rsna.org/cgi/content/full/2532082100/DC1*).

Evaluation of Kidney Function

To evaluate the size selectivity of the glomerular barrier, we intravenously injected 3000- and 70 000-Da fluorescent dextrans (Invitrogen, Eugene, Ore), conjugated with rhodamine green (maximal absorption, 502 nm; maximal emission, 527 nm) and rhodamine B (maximal absorption, 570 nm; maximal emission, 590 nm), into the ear vein at concentrations of 1 and 2 mg/mL, respectively (injected volumes, 0.125 and 0.187 mL/kg, respectively), after the first blood and urine measurements and again immediately after the sonications. To estimate the glomerular filtration rate (GFR), we calculated the creatinine clearance rate. The protein-creatinine ratio was computed with every measurement.

The fluorescence intensities of the 3000- and 70 000-Da dextrans were measured by using a fluorescent microplate reader (Gemini Fluorescent Microplate Reader; Molecular Devices, MDS Analyt-

Figure 1

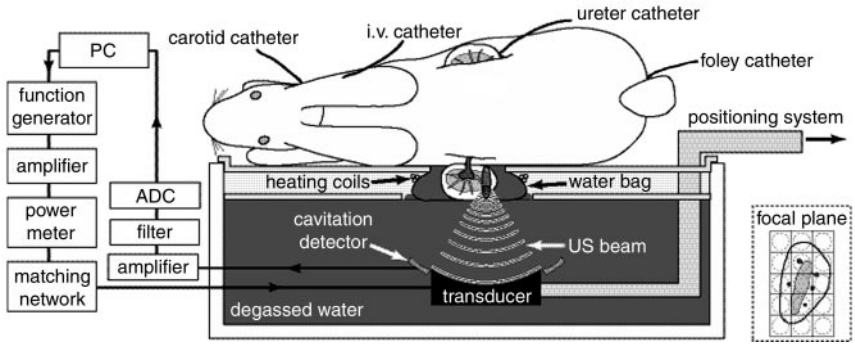

Figure 1: Diagram of experimental setup. The left kidney was exteriorized and targeted with focused US. Urine produced by this kidney was sampled from the bladder with use of a Foley catheter. The right kidney was exposed, and a ureter catheter was used to acquire urine from this kidney. Inset at bottom right shows the pattern of 15 sonication targets in the focal plane, encompassing the reservoir in which the left kidney was hanging. *ADC* = anolog-to-digital converter, *i.v.* = intravenous, *PC* = personal computer.

Figure 2

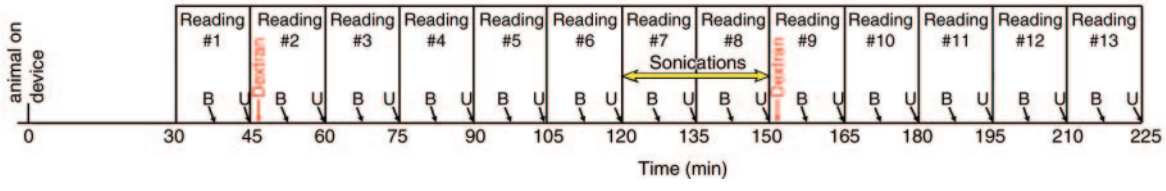

Figure 2: Timeline used in each experiment. Blood *(B)* and urine *(U)* samples were acquired at 15-minute intervals. The animal was placed on the apparatus 30 minutes before any measurements began. This interval allowed the animal to stabilize on the stage. After this time, the urine from each kidney was collected separately in test tubes. To measure the urine flow rate, the test tubes were removed every 15 minutes and replaced with empty tubes. At the midpoint of each urine collection, a 0.7-mL blood sample was taken from the carotid artery. A total of 13 measurements were obtained in each animal.

ical Technology, Toronto, Ontario, Canada). Known dilutions of the dextrans in plasma and urine were produced, and the fluorescence intensities were measured to estimate the concentrations and clearances in the experiments.

We measured the creatinine, sodium, phosphate, and urinary protein concentrations in plasma and urine and the γ-glutamyltransferase activity by using routine laboratory methods and a chemical analyzer (Hitachi 912; Roche Diagnostics, Mannheim, Germany). We estimated the tubular function by evaluating the fractional excretion of sodium, which is a measure of the percentage of sodium excreted in the urine versus the sodium reabsorbed by the kidney; the tubular reabsorption of phosphate; and the γ-glutamyltransferase–creatinine ratio. Calculation methods are described in Appendix E2 (*http://radiology.rsna.org/cgi/content/full/2532082100/DC1*).

Histologic Examination

The animals were sacrificed 1.5 hours after treatment, and their kidneys were harvested, fixed, embedded, and serially sliced. This survival time was chosen to determine the duration of the induced functional alterations. All of the treated and control kidneys were evaluated for histologic abnormalities with use of hematoxylin-eosin and periodic acid-Schiff staining every 50th and 51st slice, respectively. One author (M.K.), a renal pathologist, performed the histologic evaluations without knowledge of whether the sample was a control or treated specimen.

Data Analyses

In each animal, the relative clearance ratio (treated left kidney value/untreated right kidney value) for clearance of the fluorescent dextrans and creatinine and the urine flow rate were determined as functions of time. To test the effects of focused US treatment on these measurements, we compared the mean ratio before the treatment (mean of second to fifth measurements) with the mean ratios during and immediately after the treatment (mean of seventh to ninth measurements) and the mean ratios at a later time after the treatment (mean of 10th to 13th measurements) by using the paired *t* test. Measurement 6 was not used because in some experiments, this measurement took longer than the other measurements.

Statistical Analyses

Power analysis was applied for all groups and all parameters to justify the small sample size. In every case, the statistical power was found to be greater than 80%. The Kolmogorov-Smirnov test was used to determine if the measurements were normally distributed. We found a normal distribution of all examined parameters (clearance of creatinine and the two dextrans, urine flow rate) in each group before, during, and after the focused US treatment. To determine whether the observed enhancements in the clearances were significant, we performed paired *t* tests. Differences were considered significant at $P < .05$.

Two-way (time and power level) analysis of variance of the interaction between time and treatment was performed, with the animals nested within power level to justify the combination of the different power level groups for statistical analysis. The interactions were not significant and thus led us to conclude that we could not detect a power-dependent effect in these results. To determine the significance of the US-induced temporary effects, the mean of measurements 10–13 was compared with the baseline value (mean of pretreatment measurements 2–5) and the paired *t* test was applied to determine the significance of the difference. Statistical analysis software (SPSS; SPSS, Chicago, Ill) was used to perform the statistical analyses.

Results

Alterations in Glomerular Ultrafiltration and Permselectivity

During and immediately after focused US (measurements 7–9), 1.54-, 1.56-, and 1.70-fold elevations in the relative (treated compared with nontreated kidney) clearance of the 70 000-Da dextran were observed for the 0.4-, 0.9-, and 1.7-W treatment groups, respectively. These elevations were accompanied by 1.41-, 1.43-, and 1.63-fold increases in the urine flow rate. The ratios for relative 70 000-Da dextran clearance ($P = .046$, $P = .045$, and $P = .048$ for 0.4-, 0.9-, and 1.7-W treatment groups, respectively) and relative urine flow rate ($P = .045$, $P = .020$, and $P = .048$ for 0.4-, 0.9-, and 1.7-W treatment groups, respectively) were significantly larger than the pretreatment values (Fig 3). After focused US treatment (measurements 10–13), these ratios were not significantly different from the pretreatment values, suggesting that the effect was temporary. In five animals, no changes in relative creatinine clearance or relative 3000-Da dextran clearance were observed during or immediately after focused US. In another animal, comparatively large changes were observed: 3.00- and 2.48-fold increases in creatinine and 3000-Da dextran clearance, respectively. These six animals were considered outliers.

Enhancement was observed in the 11 remaining animals. Creatinine clearance ratios increased 1.27-, 1.28-, 1.27-fold, and 3000-Da dextran clearance ratios increased 1.35-, 1.35-, and 1.36-fold with sonications of 0.4, 0.9, and 0.7 W, respectively. The overall enhancement for both creatinine clearance and 3000-Da dextran clearance was 1.23 fold. Although enhancement ratios for the individual power levels were not significantly different from pretreatment values, when the power levels were combined, the overall enhancement was significant ($P = .04$ for relative creatinine clearance, $P = .027$ for relative 3000-Da dextran clearance) (Fig 4). This enhancement was also significant when the outliers were included. At measurements 10–13 after treatment, the clearance ratios were not significantly different from the pretreatment values. No significant changes were observed in the control animals.

Focused US treatment at 0.4 W did not result in an elevated protein-to-creatinine ratio. At 0.9 W, this ratio was elevated but still within the normal range (ie, within the range measured in the control animals). At the highest power level (1.7 W), this ratio exceeded the normal range (Fig 5). The elevated protein-to-

creatinine ratio returned to the normal range 45 minutes after the treatment ended. Although 0.4-W sonication did not elevate the fractional sodium excretion, the two higher-power-level treatments temporarily increased it: 1.32-fold in three of six cases at 0.9 W and in three of five cases at 1.7 W. Fractional sodium excretion returned to baseline 30 minutes after the treatment ended. The tubular reabsorption of phosphate and the γ-glutamyltransferase–creatinine ratio were not altered substantially at any power level. Blood pressure was stable in all cases.

Histologic Analysis

No anatomic damage at the two lower-power (0.4 and 0.9 W) levels was observed in the hematoxylin-eosin–stained sections (Fig 6). Minor tubular hemorrhage appeared after sonication at 1.7 W. No interstitial hemorrhage was seen at any power level. Periodic acid-Schiff staining revealed intact proximal tubular brush borders and normal tubular structure at every power level (Fig 6).

Acoustic Emission

Bubble activity was observed during many sonications. This activity appeared as a large increase in spectral energy at and around the resonant frequency of the passive cavitation detector (Fig 7). Emission at the harmonics of the US frequency, as well as subharmonic and ultraharmonic emissions at one-half and three-halves the US frequency, respectively, was observed. Such activity was not observed when the sonication occurred in water only or when the sonications were applied before the treatment without the microbubble contrast agent.

Discussion

We tested the hypothesis that low-power US bursts combined with a microbubble contrast agent can affect the renal barrier function. With use of sonication parameters developed to temporarily disrupt the blood-brain barrier, we observed an approximately 60% increase in the relative clearance of the 70 000-Da dextran during the focused US treatment and, on the basis of the relative clearance of two independent small-molecule agents that are freely filtered in the glomerulus (creatinine and 3000-Da dextran), a 30% elevation in glo-

Figure 3

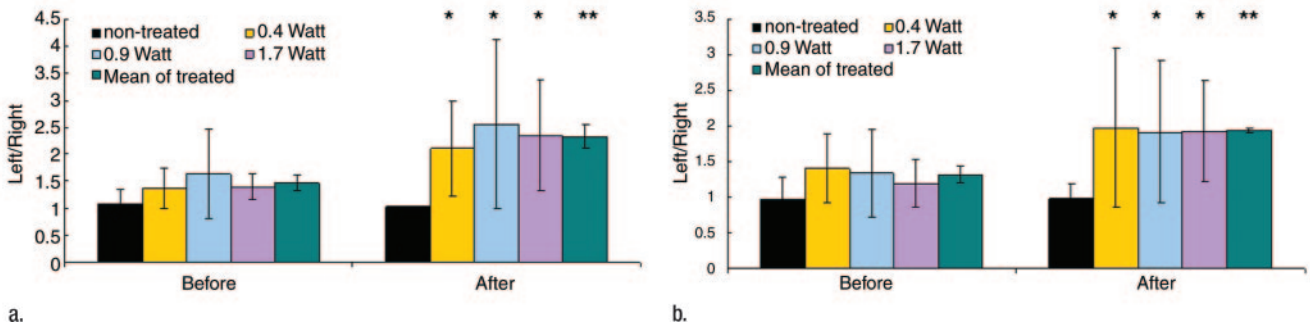

Figure 3: **(a)** Relative (left treated kidney/right control kidney) clearance of the 70 000-Da dextran and **(b)** relative urine flow rate before and after focused US treatment with microbubbles. The sonications produced significant ($P < .05$ [*], $P < .01$ [**]) enhancement ($P = .046$, $P = .045$, and $P = .048$ for relative 70 000-Da dextran clearance; $P = .045$, $P = .020$, and $P = .048$ for relative urine flow rate) that was not observed in the control animals. Mean values ± standard deviations are shown.

Figure 4

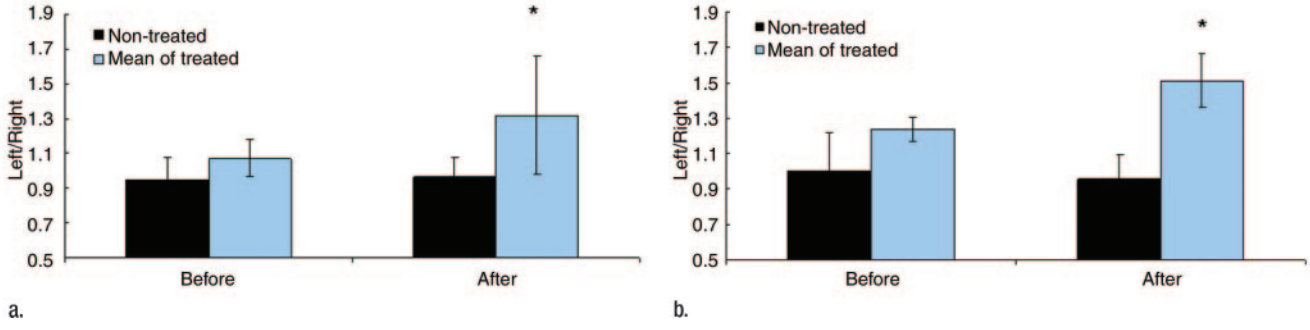

Figure 4: **(a)** Relative (left treated kidney/right nontreated kidney) creatinine clearance and **(b)** relative 3000-Da dextran clearance before and after focused US treatment with microbubbles. The sonicated regions had significant ($P < .05$ [*]) enhancement when all the treatment groups were combined ($P = .04$ for relative creatinine clearance, $P = .027$ for relative 3000-Da dextran clearance); however, enhancement in the individual groups was not significant. Mean values ± standard deviations are shown.

merular ultrafiltration. These increases in relative clearance rates started at the beginning of the focused US treatment and ended within 30 minutes of treatment completion.

The mechanisms by which US combined with the microbubble contrast agent causes glomerular ultrafiltration enhancement are not known. Several biological effects could result from the interaction between the ultrasound beam and the microbubbles and the subsequent acoustic-mechanical effects. The shelled bubbles can fragment, and the resulting free bubbles may oscillate within the acoustic field and grow by means of rectified diffusion. At sufficient acoustic pressure, they can collapse during the positive pressure cycle—a phenomenon known as inertial cavitation—and produce shock waves, high-velocity microjets, free radicals, and high local temperatures (22). Other potential effects include acoustic streaming of the fluid surrounding the bubbles, which could result in large shear stresses at the vessel walls, and a direct impulse on the vessels owing to the oscillation of the bubble or radiation force. The bubble oscillation may also produce sharp temporary pressure changes within the vessel (22). On the basis of prior brain research in which US bursts combined with similar microbubbles were used (5), we do not believe that bulk tissue heating caused the observed effects. In that work, in which heating from the exposures that disrupted the blood-brain barrier was not observed, the investigators used US parameters that were expected to produce heating greater than that induced by the low-frequency exposures used in the current study.

Figure 5

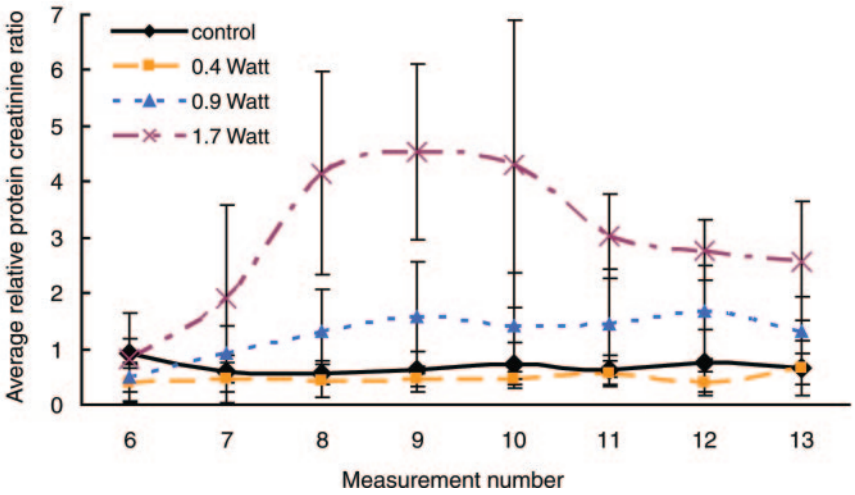

Figure 5: Relative protein-creatinine ratio as a function of time. Focused US treatment was started at measurement 7 and ended at measurement 8 (total of 13 measurements). The maximal increase in relative protein-creatinine ratio after the start of treatment was compared with the pretreatment value (measurement 6). Observed changes were significant for the 0.9-W ($P = .002$) and 1.7-W ($P = .004$) treatment groups. Means ± standard deviations are shown.

Figure 6

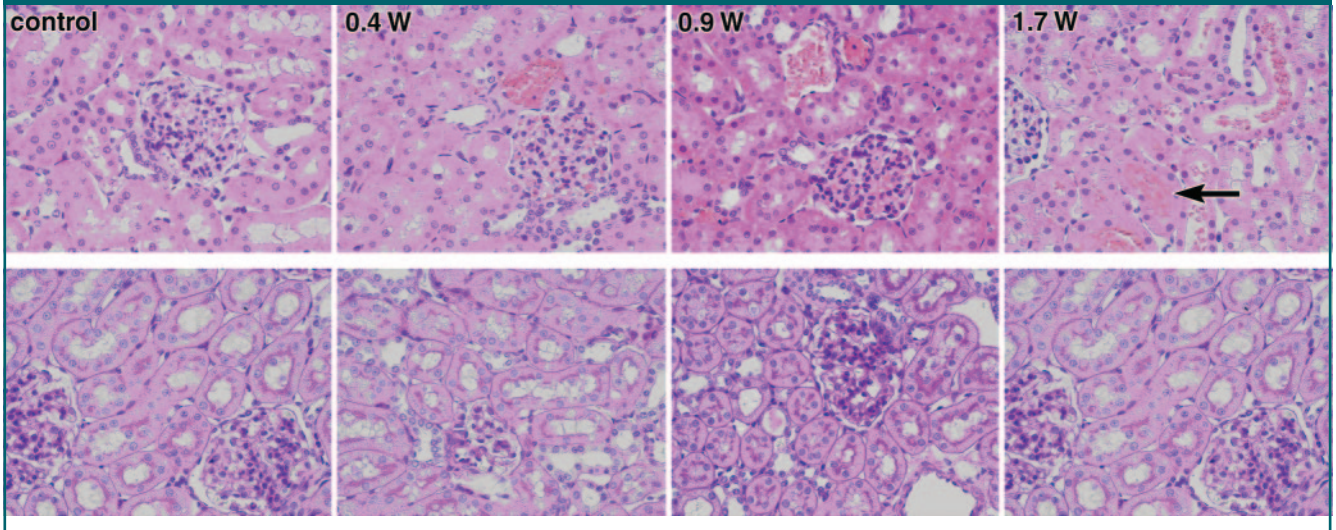

Figure 6: Microphotographs of hematoxylin-eosin–stained (top row) and periodic acid-Schiff–stained (bottom row) sections show histologic findings after focused US treatment at different acoustic power levels. At the highest power level, small tubular damage (arrow) is evident in some hematoxylin-eosin–stained sections. The periodic acid-Schiff–stained sections have a normal appearance. (Original magnification, ×60.)

The most harmful event that can be induced is inertial cavitation, which may cause hemorrhage and tissue damage (23). Neither of these events was observed at sonication power levels below the highest level tested. The fact that interstitial hemorrhage was not observed at all perhaps suggests that inertial cavitation was not dominant. However, some enhanced acoustic emission at the resonant frequency of our hydrophone, consistent with wideband emission—an indicator of inertial cavitation—was observed. This interpretation may have been confounded by ultraharmonic emission at five-halves the US frequency, which was the same as the resonant frequency of our detector. Such emission was probably present since ultraharmonic emission at three-halves the US frequency was also observed. Future research with a different cavitation detector will be necessary to determine whether the observed emission was wideband emission, which is indicative of inertial cavitation, or ultraharmonic emission, which is indicative of stable cavitation. Previous brain research suggests that inertial cavitation is not necessary to produce blood-brain barrier disruption (24–26), so if the same mechanisms are involved in GFR enhancement, cavitation may not be necessary.

Regardless of the mechanism, the capability of the sonicated kidneys to clear the 70 000-Da dextran and the rapid onset of this clearance suggest that the sonications changed the glomerular membrane properties. Previous study investigators who examined the permselectivity of the glomerular membrane and the sieving of different-size dextrans found that the filtration of the 70 000-Da dextran to the urinary space was extremely limited under normal circumstances (27,28).

It is also possible that the sonications triggered a physiologic response from the glomerular barrier that included a temporary increase in glomerular filtration. This effect might be related to vasoconstrictor stimulation of the efferent arteriole and/or to vasodilatation of the afferent arterioles.

Results of relatively recent studies of healthy animals suggest that the glomerular ultrafiltration coefficient can dynamically change as a function of time to ensure filtration pressure equilibrium and glomerular ultrafiltration stability (15,29). It was also shown in vitro that the epithelial layer of the glomerular basement membrane has a contractile phenotype in response to physiologic stimuli such as mechanical stress. This observation in vitro can mirror a capability in vivo that may influence glomerular basement membrane permeability and glomerular ultrafiltration (26).

Although increases in the kidney's filtration, urine flow, and clearance of a large-molecule agent were significant and not observed in the control animals, the results were highly variable. This variability might simply reflect the targeting uncertainty in these experiments, which were not imaging guided, or interindividual variability. Depending on the position of the kidney with respect to our grid of sonication locations, different percentages of the kidney volume could have been targeted in different animals. Also, it may be difficult to achieve substantial increases in these effects in healthy kidneys, and it is possible that the treated kidneys that showed only minor enhancement had filtration pressures close to their equilibrium value and thus could not manifest further increases. This difficulty could explain the "all or nothing" responses that seemed to occur. The variability in our results, along with the small sample sizes of the treatment groups, also may explain why the filtration enhancement did not appear to have a clear dependence on the acoustic power.

Proteinuria did appear to be influenced by the acoustic power and was not present at the lowest level tested. Sonication at only the highest power level resulted in proteinuria involving a protein-creatinine ratio in the abnormal range. At 45 minutes after treatment, however, urine protein levels returned to the normal range. This finding may indicate that excessive exposure levels are associated with a risk of tubular injury.

The fact that the fractional sodium excretion changes were transient and occurred at the highest acoustic power level only, without accompanying changes in tubular reabsorption of phosphate or urinary γ-glutamyltransferase–creatinine excretion, suggests that we induced a functional change rather than persisting structural damage. Overall, the increased creatinine clearance coupled with minimal, transient functional tubular changes suggests that the sonications induced enhancement of the GFR. However, future research should be conducted to confirm that the sonications do not cause podocyte detachment from the basement membrane of the glomerulus or endothelial cell damage that is not visible at light

Figure 7

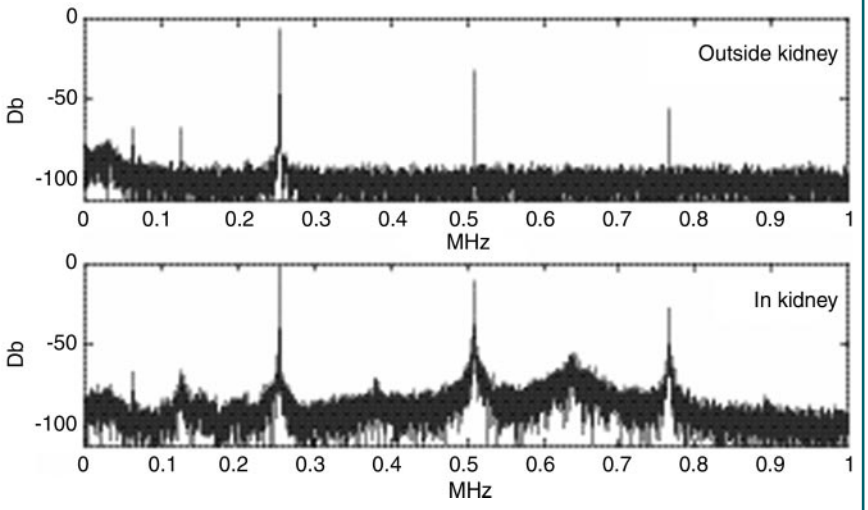

Figure 7: Measurement of acoustic emission during sonication. Spectra were acquired during pulses delivered at two locations: one site without evident bubble activity (in water) and one with wideband emission.

microscopy. Such temporary damage could explain the observed clearance of the large-molecule dextran.

Despite these promising findings, this feasibility study had several limitations. As mentioned earlier, the sonications were performed without imaging guidance, which could have ensured precise targeting of the ultrasound beam on the renal cortex. Thus, the lack of imaging guidance may have caused the variability in results that we observed. Also, we needed to exteriorize the kidney because imaging guidance was not used, and this may have influenced the results. Furthermore, the sonication parameters were not optimized, and further enhancements in the GFR may be possible. Studies should be performed to verify that the microbubbles are needed to produce the effect. Survival studies should also be performed to ensure that focused US treatment does not cause delayed effects. Finally, future research is necessary to determine whether the effects that we observed are possible in injured or diseased kidneys.

The glomerular membrane has a fundamental role in filtration impairment (27–34). A decrease in glomerular ultrafiltration is thought to originate from decreased hydraulic permeability of the capillary wall (ie, a substantial decrease in the glomerular ultrafiltration coefficient), a decreased surface area within the glomerulus, a decreased number of functioning glomeruli, or some combination of these factors (35,36). These changes may have a profound effect on the changes that can be induced with US.

In conclusion, these study results show that US bursts combined with microbubbles can temporarily enhance glomerular ultrafiltration and temporarily enable the passage of large-molecule agents that are normally not filtered by the kidney. Further improvements are possible with optimized US parameters and appropriate imaging guidance.

Practical applications: A treatment strategy that has not been tested yet is to use a mechanical stimulus highly targeted at the glomeruli to increase the glomerular ultrafiltration by either directly modifying the membranes involved in ultrafiltration or otherwise triggering a vasoactive response. Such a stimulus would be a powerful tool that leads to opportunities for novel renal therapies and a new method of studying kidney function and disease. The potential applications of this treatment would be targeted at patients with chronic kidney function impairment and/or patients without renal disease who could benefit from a GFR increase. For example, patients with severe heart failure who are resistant to conventional kidney therapies have high 1-year mortality (37). Noninvasively increasing the GFR in these patients would induce a gradual removal of excess water and salt without compromising blood pressure and could help reverse sympathetic and rennin-angiotensin overactivity. Use of this method might also generate a temporary time window in which to increase the filtration of even large-molecule substances that are normally not cleared from the kidney—for example, toxins such as Shiga toxin that are produced during *Escherichia coli* O157:H7 infection. Presumably, focused US treatment could also enhance the efficiency of the detoxification of smaller-molecule agents, such as lithium, by inducing a temporary GFR increase.

Acknowledgments: The authors are grateful to Joseph V. Bonventre, MD, PhD, for his suggestions and critical discussions. We also thank Kathleen Hasselblatt, BSc, who helped with the experiments.

References

1. Kinoshita M, Hynynen K. A novel method for the intracellular delivery of siRNA using microbubble-enhanced focused ultrasound. Biochem Biophys Res Commun 2005;335(2):393–399.
2. Dittmar KM, Xie J, Hunter F, et al. Pulsed high-intensity focused ultrasound enhances systemic administration of naked DNA in squamous cell carcinoma model: initial experience. Radiology 2005;235(2):541–546.
3. Huber PE, Pfisterer P. In vitro and in vivo transfection of plasmid DNA in the Dunning prostate tumor R3327-AT1 is enhanced by focused ultrasound. Gene Ther 2000;7(17):1516–1525.
4. Ferrara K, Pollard R, Borden M. Ultrasound microbubble contrast agents: fundamentals and application to gene and drug delivery. Annu Rev Biomed Eng 2007;9:415–447.
5. Hynynen K, McDannold N, Vykhodtseva N, Jolesz FA. Noninvasive MR imaging-guided focal opening of the blood-brain barrier in rabbits. Radiology 2001;220(3):640–646.
6. Hynynen K, McDannold N, Sheikov NA, Jolesz FA, Vykhodtseva N. Local and reversible blood-brain barrier disruption by noninvasive focused ultrasound at frequencies suitable for trans-skull sonications. Neuroimage 2005;24(1):12–20.
7. Hynynen K, McDannold N, Vykhodtseva N, et al. Focal disruption of the blood-brain barrier due to 260-kHz ultrasound bursts: a method for molecular imaging and targeted drug delivery. J Neurosurg 2006;105(3):445–454.
8. Choi JJ, Pernot M, Small SA, Konofagou EE. Noninvasive, transcranial and localized opening of the blood-brain barrier using focused ultrasound in mice. Ultrasound Med Biol 2007;33(1):95–104.
9. Tachibana K, Uchida T, Ogawa K, Yamashita N, Tamura K. Induction of cell-membrane porosity by ultrasound. Lancet 1999;353(9162):1409.
10. Kinoshita M, McDannold N, Jolesz FA, Hynynen K. Noninvasive localized delivery of Herceptin to the mouse brain by MRI-guided focused ultrasound-induced blood-brain barrier disruption. Proc Natl Acad Sci U S A 2006;103(31):11719–11723.
11. Treat LH, McDannold N, Zhang Y, Vykhodtseva N, Hynynen K. Targeted delivery of doxorubicin to the rat brain at therapeutic levels using MRI-guided focused ultrasound. Int J Cancer 2007;121(4):901–907.
12. Sheikov N, McDannold N, Jolesz F, Zhang YZ, Tam K, Hynynen K. Brain arterioles show more active vesicular transport of blood-borne tracer molecules than capillaries and venules after focused ultrasound-evoked opening of the blood-brain barrier. Ultrasound Med Biol 2006;32(9):1399–1409.
13. Raymond SB, Skoch J, Hynynen K, Bacskai BJ. Multiphoton imaging of ultrasound/Optison mediated cerebrovascular effects in vivo. J Cereb Blood Flow Metab 2007;27(2):393–403.
14. Kobori H, Nangaku M, Navar LG, Nishiyama A. The intrarenal renin-angiotensin system: from physiology to the pathobiology of hypertension and kidney disease. Pharmacol Rev 2007;59(3):251–287.
15. Deen WM, Lazzara MJ, Myers BD. Structural determinants of glomerular permeability. Am J Physiol Renal Physiol 2001;281(4):F579–F596.
16. Daniels BS, Deen WM, Mayer G, Meyer T, Hostetter TH. Glomerular permeability

barrier in the rat: functional assessment by in vitro methods. J Clin Invest 1993;92(2):929–936.

17. Deen WM, Troy JL, Robertson CR, Brenner BM. Dynamics of glomerular ultrafiltration in the rat. IV. Determination of the ultrafiltration coefficient. J Clin Invest 1973;52(6):1500–1508.
18. Huber TB, Schermer B, Benzing T. Podocin organizes ion channel-lipid supercomplexes: implications for mechanosensation at the slit diaphragm. Nephron Exp Nephrol 2007;106(2):e27–e31.
19. Hynynen K, Vykhodtseva NI, Chung AH, Sorrentino V, Colucci V, Jolesz FA. Thermal effects of focused ultrasound on the brain: determination with MR imaging. Radiology 1997;204(1):247–253.
20. McDannold N, Vykhodtseva N, Hynynen K. Blood-brain barrier disruption induced by focused ultrasound and circulating preformed microbubbles appears to be characterized by the mechanical index. Ultrasound Med Biol 2008;34(5):834–840.
21. Hynynen K. Biophysics and technology of ultrasound hyperthermia. In: Gautherie M, ed. Methods of external hyperthermic heating. New York, NY: Springer-Verlag, 1990.
22. O'Brien WD Jr. Ultrasound-biophysics mechanisms. Prog Biophys Mol Biol 2007;93(1–3):212–255.
23. Price RJ, Skyba DM, Kaul S, Skalak TC. Delivery of colloidal particles and red blood cells to tissue through microvessel ruptures created by targeted microbubble destruction with ultrasound. Circulation 1998;98(13):1264–1267.
24. McDannold N, Vykhodtseva N, Hynynen K. Targeted disruption of the blood-brain barrier with focused ultrasound: association with cavitation activity. Phys Med Biol 2006;51(4):793–807.
25. Sheikov N, McDannold N, Vykhodtseva N, Jolesz F, Hynynen K. Cellular mechanisms of the blood-brain barrier opening induced by ultrasound in presence of microbubbles. Ultrasound Med Biol 2004;30(7):979–989.
26. Sheikov N, McDannold N, Sharma S, Hynynen K. Effect of focused ultrasound applied with an ultrasound contrast agent on the tight junctional integrity of the brain microvascular endothelium. Ultrasound Med Biol 2008;34(7):1093–1104.
27. Chang RL, Deen WM, Robertson CR, et al. Permselectivity of the glomerular capillary wall: studies of experimental glomerulonephritis in the rat using neutral dextran. J Clin Invest 1976;57(5):1272–1286.
28. Toma I, Kang JJ, Peti-Peterdi J. Imaging renin content and release in the living kidney. Nephron Physiol 2006;103(2):p71–p74.
29. Friedrich C, Endlich N, Kriz W, Endlich K. Podocytes are sensitive to fluid shear stress in vitro. Am J Physiol Renal Physiol 2006;291(4):F856–F865.
30. Salmon AH, Toma I, Sipos A, et al. Evidence for restriction of fluid and solute movement across the glomerular capillary wall by the subpodocyte space. Am J Physiol Renal Physiol 2007;293(6):F1777–F1786.
31. Deen WM, Maddox DA, Robertson CR, Brenner BM. Dynamics of glomerular ultrafiltration in the rat. VII. Response to reduced renal mass. Am J Physiol 1974;227(3):556–562.
32. Drumond MC, Deen WM. Structural determinants of glomerular hydraulic permeability. Am J Physiol 1994;266(1 pt 2):F1–F12.
33. Squarer A, Lemley KV, Ambalavanan S, et al. Mechanisms of progressive glomerular injury in membranous nephropathy. J Am Soc Nephrol 1998;9(8):1389–1398.
34. Spassova MA, Hewavitharana T, Xu W, Soboloff J, Gill DL. A common mechanism underlies stretch activation and receptor activation of TRPC6 channels. Proc Natl Acad Sci U S A 2006;103(44):16586–16591.
35. Fogo AB. Mechanisms of progression of chronic kidney disease. Pediatr Nephrol 2007;22(12):2011–2022.
36. Pagtalunan ME, Miller PL, Jumping-Eagle S, et al. Podocyte loss and progressive glomerular injury in type II diabetes. J Clin Invest 1997;99(2):342–348.
37. Levy J, Morgan J, Brown E. Oxford handbook of dialysis. 2nd ed. New York, NY: Oxford University Press, 2005; 304.